



Tenofovir/Cyanovirin-N Hydrogel Formulations: An Investigation Into Rheology, Drug Release Kinetics and Mucoadhesive Properties

Karamot O. Oyediran^{1*}, Ibilola M. Cardoso-Daodu¹, Peace-Ofonabasi O. Bassey¹, Deborah A. Ogundemuren¹, Chukwuemeka P. Azubuike¹, Rachna Agarwal^{2,3}, Kondoru Haritha^{2,3}, Margaret. O. Ilomuanya^{1,4}

¹Department of Pharmaceutics and Pharmaceutical Technology, Faculty Of Pharmacy, University of Lagos, PMB 12003, Lagos, Nigeria

²Bhabha Atomic Research Centre, Mumbai, 400085, India.

³Homi Bhabha National Institute, Training School Complex, Anushaktinagar, Mumbai, 400 094, India.

⁴MEDAFRICA GMP Laboratory, Faculty of Pharmacy, University of Lagos, PMB 12003, Lagos, Nigeria

ARTICLE INFO

Article history:

Received 24 May 2025

Revised 30 June 2025

Accepted 10 July 2025

Published online 01 October 2025

ABSTRACT

Hydrogels are three-dimensional networks used for targeted delivery of therapeutically active compounds. Although the combined use of cyanovirin-N and tenofovir has not been studied, co-formulating tenofovir and cyanovirin-N in a hydrogel has great potential for preventing human immunodeficiency virus, herpes simplex virus, and human papillomavirus infections. Characterizing the hydrogel formulations is especially important for ensuring stability, efficacy, and safety. This study aims to assess the rheological behavior, drug release kinetics, and mucoadhesive properties of the hydrogels to optimize their suitability for vaginal use as multipurpose prevention technologies. Cyanovirin-N/tenofovir hydrogels were formulated using sodium carboxymethylcellulose and PEG 2000 polymers. A viscometer was used to analyze the rheological behavior of the hydrogels. Release kinetics were examined with the Franz cell apparatus and a 0.45 µm girded Millipore® membrane. Mucin adsorption studies were performed to evaluate mucoadhesion. Statistical analysis confirmed the reliability of all experimental methods. The hydrogels exhibited shear-thinning behavior, demonstrated by their ability to overcome yield stress (Herschel-Bulkley model R^2 0.8104-1), with varying degrees of pseudoplasticity and flow resistance. Rapid, complete release of tenofovir and cyanovirin-N was observed at 12 minutes and 5 minutes, respectively, along with high mucoadhesion ($\geq 85\%$). The release followed Korsmeyer-Peppas kinetics, indicating a super case II transport mechanism influenced by swelling, erosion, and diffusion. These properties support ease of application, therapeutic effectiveness, and patient adherence. The optimized tenofovir/cyanovirin-N hydrogel shows strong potential as an on-demand multipurpose preventative technology due to its favorable viscosity, mucoadhesion, and release profile.

Copyright: © 2025 Oyediran *et al.* This is an open-access article distributed under the terms of the [Creative Commons Attribution License](https://creativecommons.org/licenses/by/4.0/), which permits unrestricted use, distribution, and reproduction in any medium, provided the original author and source are credited.

Keywords: Cyanovirin-N, Tenofovir, Hydrogels, Release kinetics, Rheology, Mucoadhesion

Introduction

Hydrogels are polymer-based mesh networks with huge water components prepared from natural, semisynthetic, or synthetic polymers crosslinked by physical or chemical methods and usually used for controlled drug delivery ^{1,2} Hydrogels have excellent biocompatibility, and enable encapsulation of a wide range of molecules, including small molecules, nucleic acids, and high molecular weight proteins.³⁻⁵ These hydrogels can be engineered to respond to a range of external stimuli, including temperature, pH, electric fields, light, solvent composition, ionic strength, salt type, pressure, and specific biomolecules ^{6,7}. Hydrogels have also been used in tissue engineering, wound healing, environmental engineering, and human-machine interfaces.⁸

*Corresponding author. E mail: karamahtobi@yahoo.com
Tel: +2348038404430

Citation: Oyediran KO, Cardoso-Daodu IM, Bassey PO, Ogundemuren DA, Azubuike CP, Agarwal R, Haritha K, Ilomuanya M. Tenofovir/Cyanovirin-N Hydrogel Formulations: An Investigation Into Rheology, Drug Release Kinetics and Mucoadhesive Properties. Trop J Nat Prod Res. 2025; 9(9): 4167 – 4181 <https://doi.org/10.26538/tjnpr/v9i9.14>

Official Journal of Natural Product Research Group, Faculty of Pharmacy, University of Benin, Benin City, Nigeria

Transvaginal hydrogels are administered into the vaginal for local and systemic effects, however, the systemic absorption may be minimal. This ensures a significant reduction in the side effect profile and lowers the risk of developing resistance, particularly in antiretroviral formulations.⁹ However, challenges relating to the retention of hydrogels in the vagina due to washing off and gravitational effects make hydrogel development challenging for vagina use. This has necessitated the development of mucoadhesive hydrogels.¹⁰ Mucoadhesive polymers such as chitosan, hyaluronic acid, carboxymethylcellulose, alginates, hydroxyethylcellulose, and polyacrylic acid derivatives (such as carbopol and polycarbophil) have been employed. Such polymers form hydrogen and van der Waal bond with the mucin in the vaginal mucosa ensuring firm adhesion of the hydrogel to the vaginal wall.¹¹ Cyanovirin N (CV-N), a 101 amino acid lectin derived from the *Cyanobacterium Nostoc ellipsosporum* which has demonstrated potency against several enveloped viruses, including multiple strains of HIV, simian immunodeficiency virus, human papillomavirus, herpes simplex, Ebola, influenza, and hepatitis C.¹² Studies have demonstrated the efficacy of CV-N against HIV and Herpes simplex virus (HSV).^{13,14} CV-N binds to the high mannose oligosaccharides on viral glycoproteins gp 120 and gp 41 which are located on viral envelopes, preventing the fusion and entry of the virus into the host cells.¹⁵ This selective antiviral mechanism underscores its suitability for vaginal applications where maintaining mucosal integrity is critical. Previous studies have proven CV-N is nontoxic to tissue culture cells even at very high concentrations.¹⁶ Tenofovir (TFV), chemically called 9-[R] 2[[bis[(isopropoxycarbonyl)oxy] methoxy]

phosphonyl] methoxy] propyl] adenine fumarate, is a nucleotide reverse transcriptase clinically used with other antiretrovirals for the management of HIV infection.¹⁷ Research has also demonstrated its efficacy in the management of herpes simplex virus (HSV) and hepatitis.¹⁴⁻¹⁷ Studies have shown that vaginal tenofovir gels are well-tolerated, with minimal systemic absorption, which significantly reduces the risk of systemic side effects such as nephrotoxicity.¹⁸⁻²⁰ The topical application also mitigates gastrointestinal issues commonly associated with oral administration.²¹ The 1% tenofovir gel has shown limited effectiveness in preventing HIV and HSV in human studies, with reported success rates of 39% and 54%, respectively.¹⁸ Other multipurpose preventive technologies (MPTs) have been developed solely for HIV prophylaxis and contraception.²² This underscores the urgent need for innovative strategies and formulations that can prevent multiple sexually transmitted infections (STIs), enhancing efficacy, safety, and end-user acceptance. Sodium carboxymethyl cellulose (NaCMC) is an ionic water-soluble derivative of cellulose ether used for various hydrogel and film formulations due to its great rheological and mucoadhesive properties. Its carboxyl groups enable ionic interactions with divalent cations like calcium ions (Ca^{2+}), making it ideal for hydrogel formation. It reacts with CaCl_2 , resulting in Ca^{2+} ions crosslinking NaCMC chains through electrostatic interactions, forming a three-dimensional gel network. The ionic crosslinking increases the viscosity, mechanical strength, and swelling capacity of the hydrogel, all of which are critical for controlled drug release. The density and uniformity of this crosslinking can be modulated by adjusting the concentration of Ca^{2+} , allowing for controlled tuning of the gel's physical properties such as porosity, swelling behavior, and viscoelasticity. These parameters are critical in determining the mobility of water and solutes within the matrix, directly influencing the drug release profile.²³ TFV-bearing phosphate functional groups can be physically entrapped within the Ca^{2+} stabilized NaCMC hydrogel without chemically reacting with either the polymer or the crosslinking agent. This retention relies on non-covalent interactions such as hydrogen bonding, electrostatic forces, and spatial entrapment within the hydrogel network. The mechanism aligns with findings from NaCMC-based film systems and demonstrates the hydrogel's capacity to serve as a biocompatible carrier for controlled TFV delivery.²⁴ While some weak ionic or ion-dipole interactions may occur between the phosphate moieties of tenofovir and the divalent calcium ions, these are not strong covalent bonds that delay release. In contrast, (CV-N), a hydrophilic, cationic protein has a net positive charge at physiological to slightly acidic pH, due to the presence of lysine and arginine residues. When incorporated into a NaCMC matrix crosslinked with Ca^{2+} , CV-N is likely to interact electrostatically with the polymer chains. However, the divalent calcium ions (Ca^{2+}) crosslink NaCMC by binding to its carboxyl groups, which reduces the availability of these groups for electrostatic interaction with CV-N. Furthermore, Ca^{2+} may compete with CV-N for binding sites on the NaCMC backbone or form weak coordination complexes with CV-N itself. The nature of the interactions within the NaCMC- CaCl_2 hydrogel system has profound implications for the stability and release of TFV and CV-N.²⁵ Although the combined use of CV-N and tenofovir as a MPT has not been investigated, coformulation of tenofovir and CV-N in a hydrogel appears promising as this multipurpose preventive technology (MPT) has immense potential for prophylaxis of HIV, herpes simplex virus and human papillomavirus infection thereby offering an advantage over available MPTs used for only HIV prophylaxis. The co-formulation of these moieties may broaden the spectrum of prophylaxis and treatment, offering several advantages such as enhanced efficacy at lower doses, which can help minimize toxicity and side effects. This approach could also improve patient compliance and reduce the risk of developing resistance to therapy, a challenge observed with existing formulations, especially when used as monotherapy. The proposed synergism between CV-N and tenofovir may further enhance the efficacy of this MPT for HIV treatment. This study aims to characterize CV-N/ TFV hydrogel formulations comprehensively, focusing on their rheological properties, drug release kinetics, and mucoadhesive properties. These characteristics are crucial for the development of effective MPTs for STIs.

Materials and Methods

Material

The following reagents were obtained commercially from the companies mentioned in the brackets. Tenofovir [Energy Chemical Ltd, India], Calcium chloride anhydrous (Klincent Laboratory, Mumbai, India), Polyethylene glycol M.W 2000 (PEG₂₀₀₀) (Maclin Pharmaceuticals, India), periodic acid (Maclin Pharmaceuticals, India), Sodium carboxymethyl cellulose (MW 700,000 Da) (Sigma- Aldrich, USA), Glycerol, methylparaben, propylparaben, bovine serum albumin (BSA), mucin, disodium hydrogen phosphate, potassium dihydrogen phosphate, sodium chloride, sodium chloride, potassium hydroxide, calcium hydroxide, lactic acid acetic acid urea, glucose and Schiff's reagent (Merck Specialty Pvt Ltd, Germany). Cyanovirin-N was purified at Bhabha Atomic Research Centre, Mumbai, India, as described by Agarwal et al, 2020.²⁶ All reagents were of analytical grade, and no further purification was needed for their use.

Preparation of stable hydrogel base

Hydrogel formulations were prepared using a novel method developed as illustrated in Table 1. Hydrogels were prepared in batches where one ingredient was varied at a time while the others were kept constant, allowing the influence of each component to be individually assessed. This approach was systematically applied to all formulation ingredients. Using a magnetic stirrer, sodium carboxymethyl cellulose (2-4%) was dissolved in distilled water. Calcium chloride (0.1-1%) was weighed and dissolved in a quantified amount of water (hydrogel A-D). An aqueous solution of 5% PEG₂₀₀₀ was added to the mixture and stirred until fully dispersed. The prepared calcium chloride solution was added and stirred for crosslinking. In a separate container, 0.05 g of both methyl and propyl paraben was dissolved in distilled water and slowly added to the mixture while stirring continuously. Glycerol 1 mL was added to the mixture and stirred until a uniform, lump-free hydrogel was formed. The pH of the hydrogels was measured, then fine-tuned using 0.01M hydrochloric acid (HCl) to pH 4.5. The prepared gel formulations were stored in a clean glass container at $25^\circ \pm 2^\circ \text{C}$. The pH of the hydrogel formulations was measured immediately, at 5, 10, 15, 20 minutes, and one hour to assess the effect of curing time on the hydrogel formulations. The viscosity of the hydrogels was also measured using a Brookfield DV2TRVTJO viscometer. Physicochemical characterization and stability studies of the hydrogels were carried out over a period of 3 months.²⁷

Preparation of tenofovir- boosted CV-N hydrogel formulations

Based on the outcome of the initial preliminary assay carried out on the hydrogel base, hydrogel formulations were prepared as shown in Table 2. TFV and CV-N were added to the PEG₂₀₀₀ and mixed with the hydrogel base. Hydrogels A-H were prepared and assessed for stability. Subsequently, hydrogels I-Y were prepared to optimize hydrogels for mucoadhesion, release, and flux. Hydrogels M, N, Q, T, and Y (control hydrogels) predicted by an artificial neural network (ANN) were employed using the method previously discussed by Oyediran et al.²⁸ to evaluate the accuracy of formulation properties during the characterization and optimization process.

Characterization of hydrogel formulations

Physicochemical evaluation

The prepared gels were visually inspected for odor, color, phase separation and formation of precipitates, and the presence of any clogs. Gels were also evaluated for their feel and optical appearance. The pH was determined using a pH meter (Mettler Toledo C231551472). The probe was calibrated with pH 4.0, 7.0, and 10 standards. All measurements were recorded in triplicate. The viscosity of the formulated gels was determined by Viscometer (Brookfield DV2TRVTJO) using spindles no. 3, 5, and 7 at 5.0 to 80 rpm and Torque at 25°C . Spindle sizes were selected based on hydrogel viscosity, ensuring consistency over the assay period. The hydrogel was allowed to equilibrate for 30 min at 25°C before initiating the test.

Table 1: Hydrogel formulations using sodium carboxymethyl cellulose as polymers and calcium chloride as crosslinking agent.

Ingredients (%w/v)	A	B	C	D	E	F	G	H
CN-V (%)	0.0005	0.0005	0.0005	0.0005	0.0005	0.0005	0.0005	0.0005
Tenofovir (%)	1	1	1	1	1	1	1	1
NaCMC (%)	2	4	6	8	4	4.5	5	5.5
PEG ₂₀₀₀ (%)	5	5	5	5	2	3	4	5
Glycerol (%)	1	1	1	1	1	1	1	1
Propylparaben (%)	0.05	0.05	0.05	0.05	0.05	0.05	0.05	0.05
Methylparaben (%)	0.05	0.05	0.05	0.05	0.05	0.05	0.05	0.05
Calcium chloride (%)	0.1	0.5	0.8	1	0.1	0.5	0.8	1
Distilled water to	100	100	100	100	100	100	100	100
Dil HCl to 4.5	q. s	q. s	q. s	q. s	q. s	q. s	q. s	q. s

Stability Measurement

The potential of Hydrogen (pH), viscosity, was measured to assess the stability of the hydrogels with samples taken at scheduled time intervals (day 1, 5, 21, 60, and 90) during a 3-month storage at $25^{\circ} \pm 2^{\circ}\text{C}/65 \pm 5\%$ RH and $40^{\circ} \pm 2^{\circ}\text{C}/75 \pm 5\%$ RH according to the ICH guidelines. Physical stability was also monitored for any visual instability, such as fusion and aggregation.²⁹ Each experiment was performed in triplicate.

Rheometric evaluation of developed TFV/CNV hydrogels

The viscosity of the hydrogel formulations was measured using a Brookfield digital rotational viscometer (Model DV2TRVTJO) equipped with a spindle RV-7. All measurements were carried out at a temperature of $25 \pm 1^{\circ}\text{C}$. Before measurement, the samples were allowed to equilibrate for 10 minutes to eliminate temperature-related viscosity fluctuations. The hydrogel sample of 500 mL was carefully transferred into a clean sample beaker, ensuring the absence of air bubbles. The spindle was lowered into the sample until it was properly immersed as indicated by the instrument's immersion mark. Viscosity measurements were taken at varying rotational speeds (RPMs) to observe the rheological behavior of the formulation under different shear conditions, and the viscosity (in centipoise, cP) was recorded at each speed after stabilization. Measurements were performed in triplicate, and the average viscosity values were reported. The shear rate was estimated for each RPM using the standard shear rate chart provided for Brookfield spindles, corresponding to the spindle type and the DV2T model.

The data obtained was fitted into different models (Bingham, Power Law, and Herschel–Bulkley) to highlight the shear stress–shear rate relationships and evaluate the flow properties of the hydrogels.^{30, 31}

Mucoadhesion

The mucoadhesive test of the prepared hydrogels was measured by mucin adsorption (porcine stomach type II) and the periodic acid/Schiff colorimetric method.³² Mucin 12.5, 6.25, 3.125, and 1.625 mg per 100 mL solution in phosphate-buffered saline PBS pH 5.5 was prepared, and 200 μL of 10% periodic acid was added to 2 mL of each prepared sample and subsequently incubated for 2 h. Schiff reagent 200 μL was subsequently added to the mixture and absorbance read at 555 nm using a UV/Visible spectrophotometer (VWR, UV-6300PC Double beam), after 30 min. A plot of the absorbance versus concentration was made to obtain the calibration curve. The prepared hydrogels were mixed with mucin (dissolved in simulated vaginal fluid (SVF)) at a ratio of 1:1. The suspensions were mixed on a magnetic stirrer for 30 minutes followed by centrifugation at 400 rpm for 120 sec. The supernatant was recovered, and periodic acid 0.2 mL added to 1 mL of the supernatant with subsequent incubation at 37°C for 2 hours.³³ Schiff reagent 0.2 mL was added and incubated at 25°C for 30 min. Control hydrogels (M, N, Q, T, and Y with the same formulation parameters were used to validate results for accuracy. The absorbance was measured at 555 nm, and the mucin content was calculated from the standard calibration

curve. Each experiment was performed in triplicate, with mucin adsorption computed using equation 1

% Mucin adsorption

$$= \frac{\text{Total mass of mucin} - \text{free mucin}}{\text{Total mass of mucin}} \times 100 \quad (1)$$

In vitro drug permeability and Flux of Tenofovir and Cyanovirin-N

Simulated vaginal fluid was prepared according to the method by Owen & Katz, 1999.³⁴ The experiment used the Franz[®] diffusion cells with an available diffusional cross-sectional area of 0.98 cm^2 . A $0.45\text{ }\mu\text{m}$ white girded synthetic Millipore[®] membrane (CAT. NO. HAWG047S6, LOT. NO. F0JB71372C). A pH 4.5 simulated vaginal fluids (SVF) was used as the receptor (kept at $37 \pm 1^{\circ}\text{C}$ in a water bath) compartment of the Franz[®] diffusion cell and filled with 25 mL of SVF. Hydrogel formulations 1 g were placed on a membrane that had been pre-soaked overnight in simulated vaginal fluid (SVF). 2 mL samples were withdrawn from the receptor medium into sterile sample bottles for analysis at varying time intervals. The concentrations of TFV in the permeant at varying time lapses were measured with a UV/ VIS spectrophotometer at 260nm.³⁵ Measurements were taken in triplicate, and a plot of concentration permeated against time was plotted. The drug flux at a steady state ($J_{ss}\text{ }\mu\text{g}/\text{cm}^2/\text{h}$) was calculated from the slope of the linear portion of the cumulative amount permeating the membrane per unit area versus time plot. For Cyanovirin-N, concentration was measured by subjecting the SVF retrieved from the receptor compartment at various time intervals to the Folin Lowry assay for proteins.³⁶ Control hydrogels M, N, Q, T, and Y with the same formulation parameters were used to validate results for accuracy. The experiment was performed in triplicate.

For the Folin-Lowry assay, an alkaline sodium carbonate solution was prepared by dissolving sodium bicarbonate NaHCO_3 , 20 g, in 0.1mol/L sodium hydroxide (NaOH). Copper sulfate sodium–potassium tartrate solution was freshly prepared by mixing hydrated copper sulfate $\text{CuSO}_4 \cdot 5\text{H}_2\text{O}$ 5 g in 10 g/L sodium–potassium tartrate. Alkaline sodium carbonate solution 50 mL was mixed with Copper sulfate sodium–potassium tartrate solution, 1 mL. The folin ciocalteu reagent was freshly diluted with an equal volume of water before use. To SVF (1 mL) retrieved from the receptor compartment at various time intervals, alkaline solution 5 mL was added to each test tube and mixed thoroughly. The solution was allowed to stand at room temperature for 10 minutes. Diluted Folin-Ciocalteu reagent 0.5 mL was added, mixed thoroughly and allowed to stand for 30 minutes. The absorbance was measured at 750 nm. CV-N standard ($2.5\text{--}120\text{ }\mu\text{g}/\text{mL}$) in SVF and the blank solution were also subjected to the same procedure. A standard curve was constructed, and the concentration of CV-N in the SVF at various time intervals was extrapolated from the standard curve.³⁶

Statistical Analysis

Data obtained were documented as mean \pm SD (standard deviation). Stability data (pH, viscosity) were subjected to ANOVA to test if there was a significant difference in the data obtained. P-values ≤ 0.05 were

considered statistically significant. Tukey's Honestly Significant Difference (HSD) post-hoc test was used after an ANOVA to identify which specific group means are significantly different.

Results and Discussion

Physicochemical characterization of hydrogels

All Hydrogel formulations were off-white, homogenous, and smooth except for hydrogel D and H, which were extremely viscous and stiff. The odor was agreeable; hydrogels were easily spread and easy to wash

off with water. The increase in viscosity observed was consistent with increased polymer concentration. The pH of the hydrogel formulations ranged from 4.47 ± 0.01 to 4.48 ± 0.01 . All hydrogels show clear shear-thinning behavior, where viscosity decreases as shear rate increases. However, a significant decline in multipoint viscosity was observed in formulations A-C by day 7. Hydrogel D, which was extremely viscous on day 1 with lumps, was observed to be homogenous on day 7 with no lumps (Table 3). The viscosity of other hydrogels remained consistent over the assay period (Figure 1).

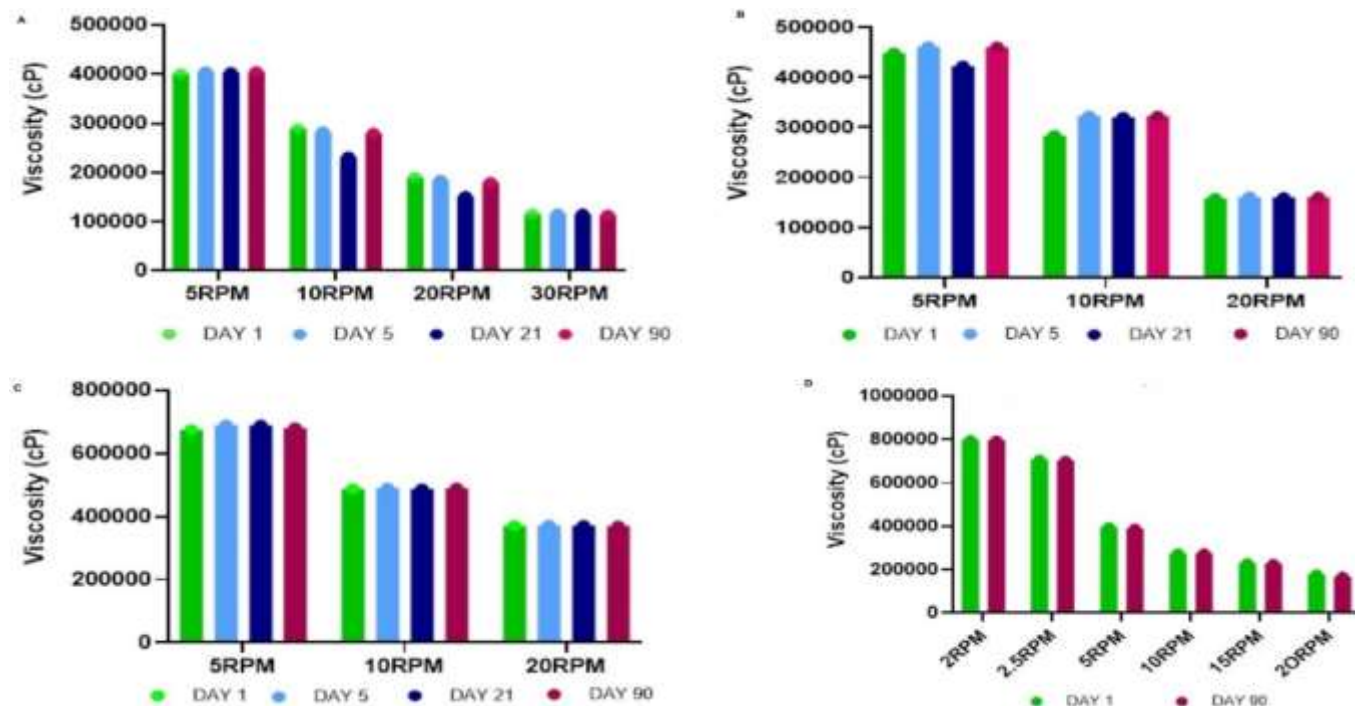


Figure 1: Viscosity of hydrogels measured at varying RPM over a period of 3 months (A) Hydrogel E (B) Hydrogel F (C) Hydrogel G (D) Optimized hydrogel

The rigidity of hydrogel D and H can be attributed to the extremely high concentration of the polymer NaCMC and crosslinker, typical of highly crosslinked hydrogels resulting in excessive Ca^{2+} ions crosslinking NaCMC chains through electrostatic interactions, forming a stiff gel network.³⁷ All hydrogels had an agreeable odor, were easily spread, and easy to wash off with water. An increase in viscosity observed was consistent with increased polymer concentration as highlighted in Table 3. The reduction in viscosity with increased shear rate highlighted the pseudoplastic nature of the hydrogels, demonstrating reversible disruption and reformation of their internal network structure under applied stress typical of crosslinked hydrogels. The interaction of the divalent calcium ions (Ca^{2+}) with two negatively charged carboxylate groups on separate NaCMC chains forms ionic crosslinks capable of reformation of the hydrogel network on application and removal of shear stress.³⁸ The pH of the hydrogel formulations ranged from 4.47 ± 0.01 to 4.48 ± 0.01 making it suitable for vaginal administration. The pH was measured at intervals for up to one hour after hydrogel formation to assess the hydrogel gelation time. It revealed no substantial change in pH over the period assayed. This implies that the gelation process of these hydrogels was very rapid, occurring within the first few minutes of preparation.

Stability of hydrogel formulations

The hydrogel formulations were evaluated for their appearance, pH, and viscosity. These parameters were monitored to assess the stability of the hydrogels throughout the study period, as summarized in Table 3 and illustrated in Figure 1.

Results obtained from characterization of hydrogels A-D demonstrated no change in hydrogel color, homogeneity, and pH measured for

hydrogels A, B, and C. However, a significant decline in viscosity was evident for hydrogels A and B after 7 days. The decline observed in viscosity can be attributed to the disproportionate ratio of hydrogel polymers (NaCMC and PEG 2000). A high concentration of PEG 2000 in the hydrogels relative to the concentration of the NaCMC resulted in the mechanical softening of the gel network. Studies by Rubinson and Meuse have highlighted that at high concentrations, PEG molecules are found in groups competitively binding water molecules sparingly, spatially interfering with ionic crosslinking between polymer chains, weakening the gel matrix.³⁹ Its plasticizer effect may also result in the thinning of the hydrogel by a reduction in the storage Young modulus.⁴⁰ Lumps were noticeable in hydrogel D after preparation due to the extremely high viscosity that made mixing difficult. By day 7, the lumps were no longer observed, leaving a homogenous hydrogel. The sharp decline in viscosity may be due to an imbalance in the ratio of polymer(s) and crosslinker, calcium chloride. An insufficient polymer and/or crosslinker concentration may also contribute to the weaker hydrogel network, which degrades faster over time. Ensuring an ideal ratio of polymer and crosslinker concentration is crucial to preserving a balanced ratio of polymers to crosslinkers, and maintaining consistent crosslinking conditions is crucial for preserving the structural integrity and viscosity of hydrogels over time.⁴¹ The high concentration of PEG 2000 used with low concentration of NaCMC, resulted in excessive decline in viscosity of the hydrogels due to the plasticizer nature of PEG 2000 resulting in thinning and breakdown of the hydrogels over a short period as observed in hydrogels A and B. Excessively high crosslinker concentration can also result in an extremely rigid hydrogel matrix which can eventually become brittle and degrade over time.⁴² This trend was observed in hydrogel D, which combines a high concentration of crosslinker and NaCMC.

Table 2: Composition of Hydrogel formulations I-Y and Optimized hydrogel.

INGREDIENTS (%w/v)	I	J	K	L	M	N	O	P	Q	R	S	T	U	V	W	X	Y	Op
CN-V (%)	0.0005	0.0005	0.0005	0.0005	0.0005	0.0005	0.0005	0.0005	0.0005	0.0005	0.0005	0.0005	0.0005	0.0005	0.0005	0.0005	0.0005	0.0005
Tenofovir (%)	1	1	1	1	1	1	1	1	1	1	1	1	1	1	1	1	1	1
NaCMC (%)	4.5	5	4	4.5	4.5	4.5	5	4.5	4.5	4	4	4.5	5	5	4.5	4	4.5	4
PEG 2000(%)	2	2	3.5	2	3.5	3.5	3.5	5	3.5	2	3.5	3.5	3.5	5	5	5	3.5	2
Glycerol (%)	1	1	1	1	1	1	1	1	1	1	1	1	1	1	1	1	1	1
Propylparaben (%)	0.05	0.05	0.05	0.05	0.05	0.05	0.05	0.05	0.05	0.05	0.05	0.05	0.05	0.05	0.05	0.05	0.05	0.05
Methylparaben (%)	0.05	0.05	0.05	0.05	0.05	0.05	0.05	0.05	0.05	0.05	0.05	0.05	0.05	0.05	0.05	0.05	0.05	0.05
Calcium chloride (%)	0.1	0.55	1	1	0.55	0.55	0.1	1	0.55	0.55	0.1	0.55	1	0.55	0.1	0.55	0.55	1
Distilled water to (%)	100	100	100	100	100	100	100	100	100	100	100	100	100	100	100	100	100	100
Dil HCL to 4.5	q. s	q. s	q. s	q. s	q. s	q. s	q. s	q.s	q. s	q. s	q. s	q. s	q. s	q. s	q. s	q. s	q. s	q. s

OP-Optimized hydrogel formulation. Hydrogels M, N, Q, T, and Y are control hydrogels.

Table 3: Physicochemical characterization of hydrogels A-D highlighting a drastic decline in viscosity over a 7-day period.

HYDROGEL		25° ± 2 °C / 65 ± 5% RH	
	Properties	DAY 1	DAY 7
A	Color	Clear and colorless	Clear and colorless
	Appearance	Homogenous and runny	Homogenous and runny
	pH	4.48 ± 0.01	4.47 ± 0.030
	Viscosity (cPas) 10rpm	20826.67 ± 0.65	3200 ± 0.52
B	Color	Off-White	Off-White
	Appearance	Homogenous and smooth	Homogenous and smooth
	pH	4.47 ± 0.01	4.47 ± 0.05
	Viscosity (cPas) 10rpm	288044.4 ± 0.41	75560 ± 0.11
C	Color	Off-White	Off-White
	Appearance	Homogenous and thick	homogenous and thick
	pH	4.48 ± 0.00	4.48 ± 0.04
	Viscosity (cPas) 10rpm	398790 ± 0.55	338400 ± 0.16
D	Color	Off-White	Off-White
	Appearance	Homogenous with lumps	Homogenous with no lumps but very viscous
	pH	4.48 ± 0.01	4.48 ± 0.03
	Viscosity (cPas) 10rpm	*****	*****

***** viscosity not measured **OP-Optimized hydrogel

Hydrogels E-G, I-Y, and optimized hydrogel remained stable at both temperatures $25^{\circ} \pm 2^{\circ}\text{C}$ / $65 \pm 5\%$ RH and $40^{\circ} \pm 2^{\circ}\text{C}$ / $75 \pm 5\%$ RH as the pH remained consistent at 4.5 and the viscosity remained constant with no statistically significant difference observed over the three-month study period. However, the physical breakdown of hydrogel H was observed during the three-month period. This degradation occurred due to a disproportionate ratio of polymer and crosslinker. Ensuring a balanced ratio of polymers to crosslinkers and maintaining consistent crosslinking conditions are crucial for preserving the structural integrity and viscosity of hydrogels over time.⁴³ The hydrogels exhibited shear-thinning behavior with an increasing shear rate typical of non-Newtonian fluids. This trend is common in polymeric formulations and allows for ease of administration, as well as prolonged mucosal contact in the vagina. These are crucial for the efficacy and acceptability of the formulation.⁴⁴

Rheology of hydrogel formulations

The rheological properties of hydrogel formulations were assessed using the Power Law, Bingham, and Herschel-Bulkley models (Figure 2A-I). Key parameters derived from each model fitting are presented in Table 4. The power model highlights that hydrogel samples exhibited shear-thinning behavior, as indicated by flow behavior indices (n) less than 1. The consistency indices (k) ranged from 1063.9 to 2912.6, with high coefficients of determination ($R^2 > 0.9$), confirming the suitability of the Power Law model for describing the flow behavior. Bingham model fittings revealed significant yield stresses (τ_0), varying from 1958.4 to 3676.7 Pa, suggesting that finite stress is required to initiate flow in these systems. The slope values ($1/\eta$), ranging from 36.2 to 367.5 Pa^{-1} , reflected the flow behavior following yield stress. Model fits were generally strong with R^2 0.8766–1. The Herschel-Bulkley model, which combines yield stress and non-linear flow, also provided excellent fits R^2 0.8104–1 (suppl fig), with Herschel-Bulkley n values ranging from 0.9087 to 2.7094. The apparent consistency factors (K) ranged from 7.26 to 344.67, depending on the formulation.

The rheological characterization of hydrogel formulations using the Power Law, Bingham, and Herschel-Bulkley models describes the structural behavior of the hydrogels under shear stress and at rest, hence influencing ease of use, end-user acceptance, release of TFV and CV-N, efficacy, stability and suitability for vaginal application. The Power Law model revealed moderate to high goodness-of-fit (R^2 values) and n value below 1. This highlights the non-Newtonian, shear-thinning behavior of the hydrogels, typical of polymeric systems.⁴⁵ This shear-thinning property is beneficial for application, as it allows the gel to spread easily under pressure while maintaining viscosity at rest. The Bingham model also provided a good fit, indicating that stress is necessary before flow.⁴⁶ This is essential for ensuring the gel remains in place post-application, minimizing leakage. Conversely, moderate yield stress values in formulations suggest a favorable balance between vagina retention and spreadability. However, the use of an applicator may be necessary for optimal vaginal administration. The Herschel-Bulkley model produced the best R^2 values for most, indicating hydrogels possess yield stress and shear-thinning characteristics with varying degrees of pseudoplasticity and flow resistance, indicating a complex flow behavior of the hydrogels.⁴⁷

For vaginal administration, formulations must balance spreadability with mechanical robustness to ensure ease of insertion and spreading and resist leakage while ensuring stability during storage. High pseudoplasticity (low n power law values) indicates strong shear-thinning behavior, which favors easy application under manual pressure while resisting flow at rest. However, extremely low n values can lead to overly soft gels that are unstable in situ. Hydrogels L, M, and OP had good balance ($n = 0.31$ – 0.43), with the OP hydrogel having the most favorable flow behavior combining adequate viscosity under storage to maintain hydrogel stability and retention in the vagina while ensuring hydrogel swelling and release of TFV and CV-N for efficacy. The yield stress needed to ensure flow promotes the stability of the hydrogels. High shear rates during application overcome the yield stress and reduce viscosity, facilitating easy spread and uniform coating of the vaginal epithelium whereas at low shear, viscosity increases, promoting retention and reducing leakage or gravitational flow from the vagina orifice for efficacy.

Mucin adsorption is a measure of mucoadhesion based on the interaction of the polymer with mucin during contact. This interaction is dependent on the chemical structure and the functional groups present at the surface of the moieties. The polar functional groups present rearrange at the interface, causing chemisorption as a result of hydrogen bonding or van der Waals forces.⁴⁸ Mucin is a glycoprotein that forms the protective layer of the mucosa, and its adsorption by hydrogels can affect their biocompatibility and efficacy.⁴⁹ All hydrogel formulations had percentage mucoadhesion levels of 85% and higher, apart from hydrogels A and B. This indicates a high potential of the hydrogel to adhere to the vaginal wall, prolonging contact time and facilitating drug delivery. The low mucoadhesion of hydrogels A-C can be attributed to the disproportionate ratio of the copolymer's sodium carboxyl methylcellulose and PEG 2000 with the crosslinker. Formulation G had the highest mucoadhesion (99.2%), but the optimized formulation combines high mucoadhesion (96.3%) with high flux and release of the incorporated active moieties. Sodium carboxyl methyl cellulose is an anionic polymer capable of interacting with positively charged ions in the mucin. Conversely, the concentration of NaCMC exhibited a positive influence on mucoadhesion, as indicated by the nearly linear increase in mucoadhesion values with increasing NaCMC concentration. This trend suggests that higher concentrations of NaCMC enhanced mucoadhesive properties due to the increased interaction between NaCMC and mucin.⁵⁰ Moreover, diffusion of the polymer chains into the loops in the glycoprotein mucin network and the formation of new hydrogen and other non-covalent bonds further promote mucoadhesion. PEG 2000 also influences the mucoadhesion of the hydrogel formulations as it promotes hydration of the mucosa, thereby enhancing lubrication and mucoadhesion. PEG 2000 forms hydrogen bonds with mucin through the interaction of its ether groups with mucin. Both polymers also absorb a large amount of water, causing swelling. Swelling of the polymers facilitates hydrogel mucoadhesion by increasing the surface area for interaction of the hydrogel with mucin.⁵¹ High mucoadhesion of the hydrogels has significant implications in the efficacy of the hydrogels, enhancing hydrogel retention in the vagina and promoting release of incorporated moieties for therapeutic efficacy.

Release kinetics of TFV and CV-N from hydrogel formulations

The results obtained from the release studies of TFV from the hydrogel formulations were fitted into varying release kinetic models zero order, Korsmeyer-Peppas, first order and Higuchi (Figure 4-5) to elucidate the release mechanism. The varying release constants were highlighted to assess the best model to depict the release of TFV from the hydrogel formulations (Table 5). The release pattern of tenofovir from the optimized hydrogel formulation provides further insight into the most suitable release model for TFV. The release studies of CV-N from the optimized hydrogel formulations were analyzed using various kinetic models, including zero-order, first-order, Korsmeyer-Peppas, and Higuchi (Figure 6), to elucidate the release mechanism. The corresponding release constants were evaluated to determine the most appropriate model for describing the release of CV-N from the hydrogels, as summarized in Table 6. The cumulative TFV and CV-N amount released over time per unit area was estimated.

The in-vitro release kinetics of the hydrogel formulations was carried out using the Franz cell diffusion method with simulated vaginal fluid (SVF) as the medium. SVF was used to mimic the physiological conditions in the vagina area.³⁴ The release pattern of TFV and CV-N from hydrogels was best fitted with korsmeyer peppas kinetics, despite the high R^2 value observed for other release kinetic models. This indicates a complex release pattern involving the erosion of the hydrogel matrix and breakdown, in addition to swelling and rapid diffusion through the hydrogel matrix, typical of NaCMC hydrogels.⁵¹ This is consistent with the release pattern of TFV, where an initial burst release was observed within the first 5 minutes. This rapid release phase can be attributed to hydrogel matrix erosion and swelling. This was followed by a slower, diffusion-controlled phase, within 12 minutes, as the drug gradually diffused through the hydrated polymer network toward maximum cumulative release. The complete release of TFV was observed at 12 minutes. The burst pattern release of CV-N from the hydrogel matrix due to rapid erosion and swelling of the hydrogel

matrix ensures complete release of CV-N within 5 minutes. The Peppas model highlighted that all hydrogels had a diffusion coefficient $N > 1$, indicating a non-Fickian super case II transport release mechanism, mediated by polymer relaxation-driven burst release.⁵² The Higuchi model, a model of the Korsemeyer Peppas and should not be used when the release is due to hydrogel swelling, hence the TFV release from the hydrogels cannot be described using the Higuchi model.⁵³ Whereas the first and zero order (constant rate and concentration dependent release respectively) does not align with the release pattern of TFV. The optimized hydrogel had the fastest burst release of TFV with a flux rate of $9806 \mu\text{g}/\text{cm}^2/\text{hr}$. Other hydrogel formulations also exhibited the burst release pattern with flux of $2291\text{-}5061 \mu\text{g}/\text{cm}^2/\text{hr}$.

Mucoadhesion

The percentage mucoadhesion of the hydrogel formulations was assessed to evaluate their adhesive properties under simulated physiological conditions. Figure 3 illustrates the comparative mucoadhesion profiles of formulations A to Y, alongside the optimized formulation.

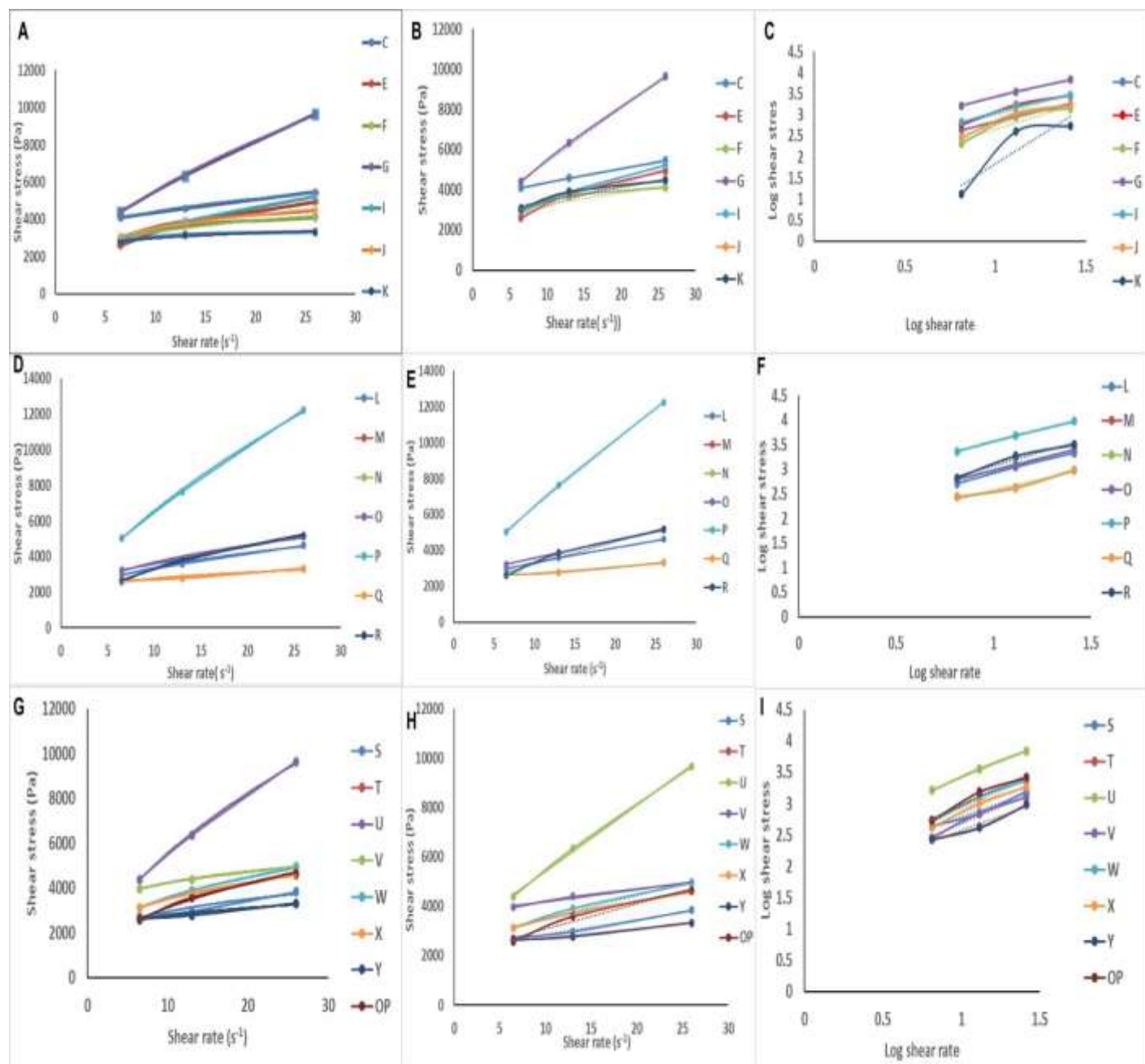


Figure 2: Rheological Characterization of Hydrogels C-K Using (A) Power (B) Bingham and (C) Herschel-Bulkley Model, Hydrogels L-R Using (D) Power (E) Bingham and (F) Herschel-Bulkley Model, and Hydrogels S-Y/ OP Using (G) Power (H) Bingham and (I) Herschel-Bulkley Model.

Table 4: Results of model fitting of Rheological characterization of hydrogel formulations

Power model				Bingham model			Herschel Bulkley model			
Hydrogel	N	K	R ²	η_p	τ_0	R ²	N	log(K)	K	R ²
C	0.2078	2744.9	0.9862	69.6	3654.7	0.999	1.023	1.8151	65.3281	0.9985
E	0.4610	1117.9	0.9926	115.5	2019.3	0.9962	1.1557	1.8718	74.4389	0.9594
F	0.2477	1871.1	0.9531	57.1	2702.1	0.8766	1.3695	1.2952	19.7333	0.8848
G	0.5684	1501.0	0.9987	267.5	2733.8	0.9982	1.032	2.3887	244.737	0.9973
I	0.4168	1341.8	0.9999	115.5	2266.6	0.9907	1.0756	1.9707	93.4756	0.9872
J	0.2749	1859.2	0.9728	68.6	2769	0.9122	1.287	1.48	30.1995	0.9111
K	0.1286	2219.1	0.9202	68.6	2769	0.9122	2.7094	0.8608	7.2577	0.8104
L	0.3178	1624.9	0.9936	83.8	2461.9	0.9978	1.0351	1.8807	75.9801	0.9969
M	0.1682	1882.3	0.9172	36.4	2359.9	0.9978	0.9087	1.6688	46.6444	0.9649
N	0.1682	1882.3	0.9172	36.4	2359.9	0.9978	0.9087	1.6688	46.6444	0.9649
O	0.3339	1704.1	0.9858	97.6	2606	1	1.0032	1.9857	96.7609	1
P	0.6409	1503.8	0.9989	367.5	2733.8	0.999	1.0231	2.5374	344.6672	0.9985
Q	0.1682	1882.3	0.9172	36.4	2359.9	0.9978	0.9087	1.6688	46.6445	0.9649
R	0.4898	1063.9	0.9949	126.7	1958.4	0.9731	1.1362	1.9362	86.3376	0.9667
S	0.2500	1654.8	0.9348	59.1	2281	0.9862	0.9198	1.866	73.4514	0.9739
T	0.1682	1882.3	0.9172	36.2	2359.9	0.9818	0.9087	1.6688	46.6445	0.9649
U	0.5684	1501	0.9987	267.5	2733.8	0.9982	1.032	2.3887	244.7372	0.9973
V	0.1627	2912.6	0.9979	50.3	3676.7	0.9875	1.0886	1.5938	39.2464	0.9832
W	0.3308	1678	0.9997	91.3	2603.6	0.9887	1.0837	1.8589	72.2603	0.9847
X	0.2756	1859	0.9991	73.0	2707.6	0.9888	1.0834	1.7622	57.8362	0.9848
Y	0.1682	1882.3	0.9172	36.4	2359.9	0.9978	0.9087	1.6688	46.6445	0.9649
OP	0.4272	1170.3	0.9955	103.2	2038.4	0.9704	1.144	1.8374	68.7702	0.9594

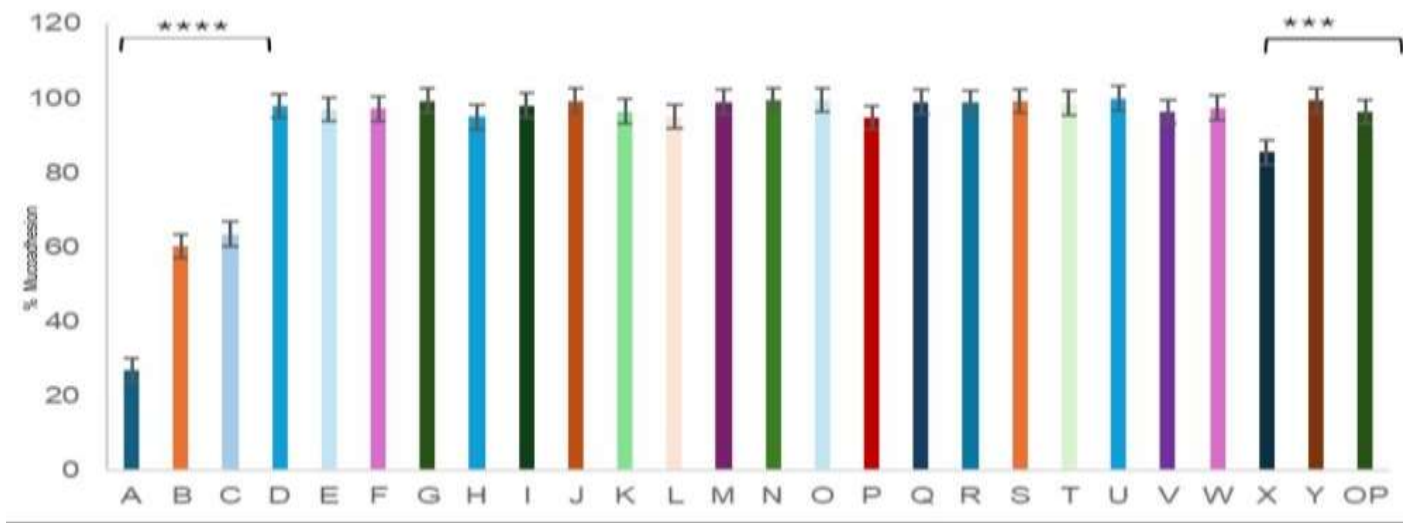


Figure 3: Percentage mucoadhesion of hydrogel formulations.

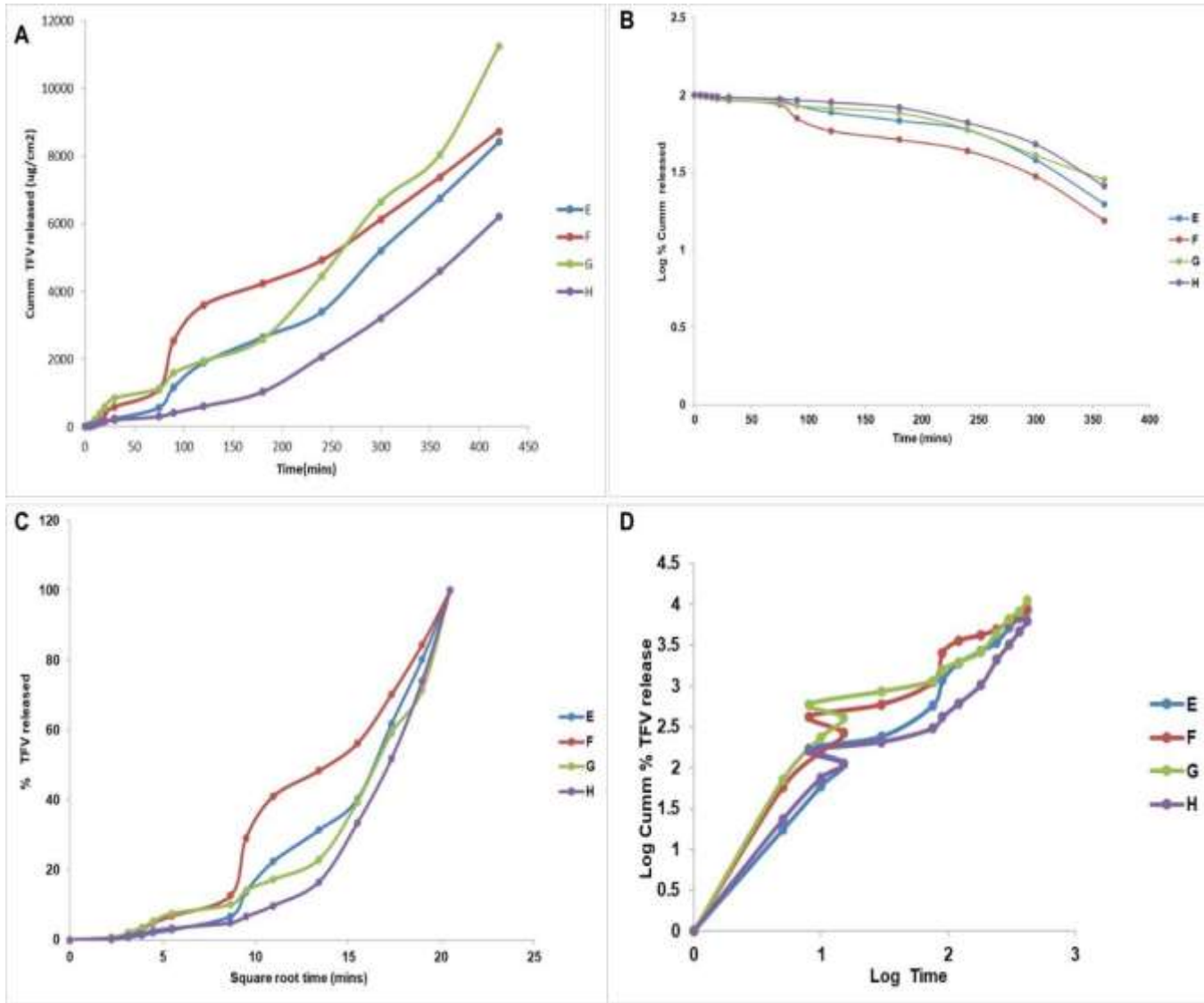


Table 5: Model fitting of release kinetics of TFV from CV-N /TFV hydrogel formulation in simulated vaginal fluid pH 4.2 Where K_0 is the release constant, R^2 is the coefficient of determination, K_H is the Higuchi release constant, N is the Higuchi dissolution constant.

Kinetic model	Parameters	E	F	G	H	I	J	K	L	M	N	O
Zero order	R^2	0.9786	0.9829	0.9579	0.923	0.9885	0.9959	0.9448	0.8869	0.9312	0.81	0.9551
	K_0	19.21	20.731	23.792	13.192	46.332	48.516	38.275	72.455	59.284	62.834	77.595
First order	R^2	0.886	0.9563	0.908	0.8258	0.7965	0.7434	0.7425	0.8787	0.9033	0.9456	0.826
	K	0.0016	0.002	0.0013	0.0013	0.0034	0.0032	0.0035	0.0036	0.0038	0.004	0.0034
Korsmeyer-Peppas	R^2	0.9639	0.9143	0.977	0.9304	0.9155	0.9959	0.9049	0.9539	0.9407	0.9303	0.9482
	N	1.3653	1.2761	1.2066	1.2052	1.4394	1.3584	1.3479	1.19	1.3841	1.4562	1.3622
Higuchi	R^2	0.8659	0.947	0.857	0.7607	0.9701	0.9404	0.8327	0.9751	0.9865	0.9291	0.9838
	K_H	3.974	4.6639	3.4902	3.2934	5.1017	4.8443	4.6561	4.7396	5.3724	5.4989	5.1676
Kinetic model	Parameters	P	Q	R	S	T	U	V	W	X	Y	OP
Zero order	R^2	0.928	0.9432	0.985	0.9267	0.9379	0.8582	0.8879	0.8914	0.8984	0.9549	0.9109
	K_0	52.53	52.152	188.42	53.552	60.948	42.356	76.668	75.928	62.001	62.311	304.08
First order	R^2	0.8476	0.8196	0.7094	0.8572	0.8667	0.8931	0.8923	0.8834	0.894	0.9083	0.9693
	K	0.0034	0.0033	0.0031	0.0035	0.0036	0.0036	0.0031	0.0035	0.0036	0.0038	0.0046
Korsmeyer-Peppas	R^2	0.9233	0.918	0.9061	0.9933	0.9624	0.9113	0.9851	0.9875	0.991	0.9368	0.9197
	N	1.2074	1.2028	1.4126	1.1774	1.2691	1.1862	1.2244	1.2237	1.2052	1.4097	1.4084
Higuchi	R^2	0.9923	0.9877	0.9049	0.9933	0.9892	0.9689	0.9831	0.9846	0.9857	0.9895	0.9688
	K_H	4.9189	4.7493	4.5982	4.8502	5.0556	4.9961	4.9671	4.9644	4.937	5.3723	5.6667

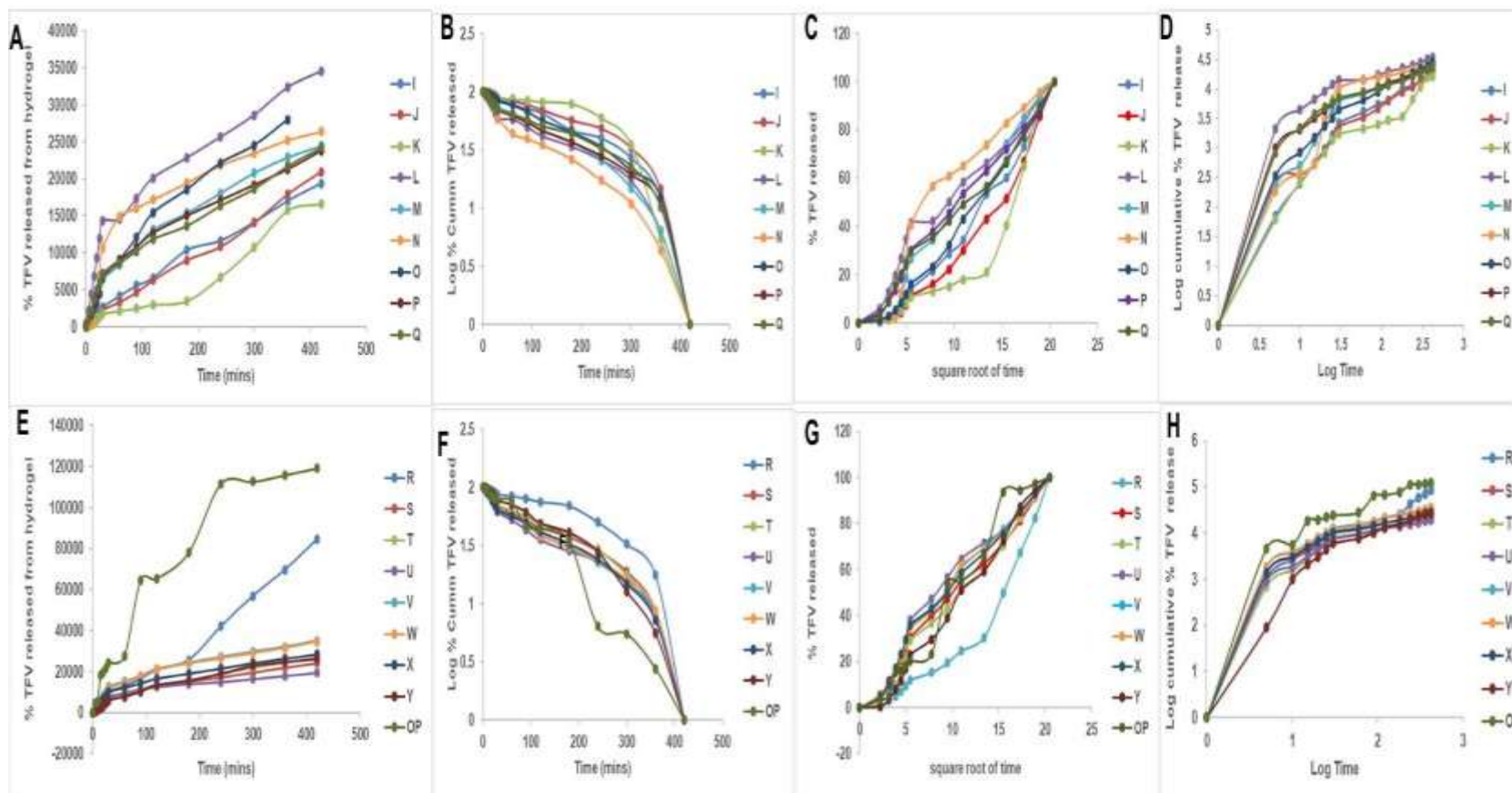


Figure 5: Release models of I-Q(A) Zero order (B) First order (C) Higuchi (D) Korsmeyer-peppas of tenofovir from hydrogel formulations. Release models R-Y/Optimized (E) Zero order (F) First order (G) Higuchi (H) Korsmeyer-peppas of tenofovir from hydrogels R-Y and Optimized hydrogel.

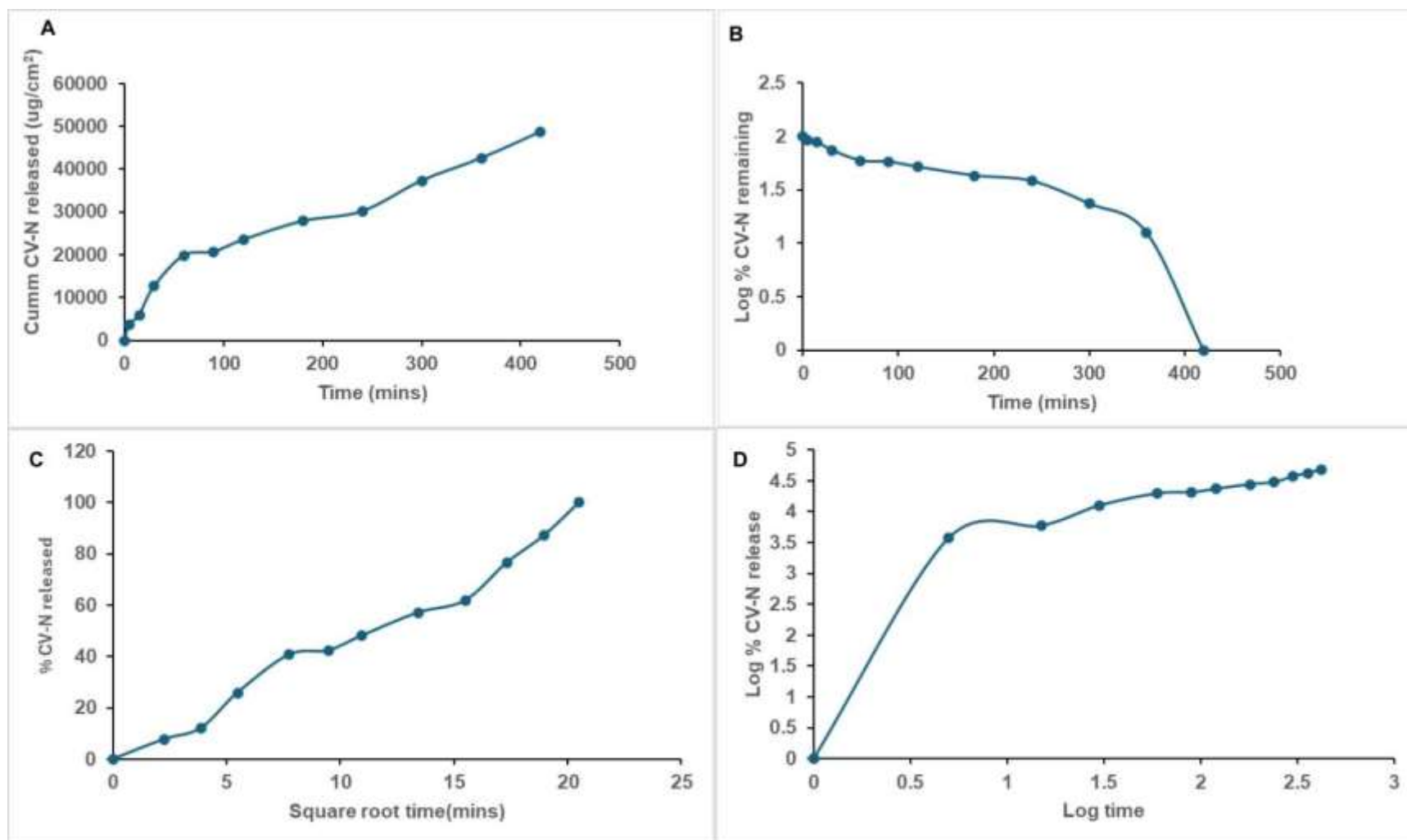


Figure 6: Release models(A) Zero order (B) First order (C) Higuchi (D) Korsmeyer-peppas of CV-N from optimized CV-N/TFV hydrogel

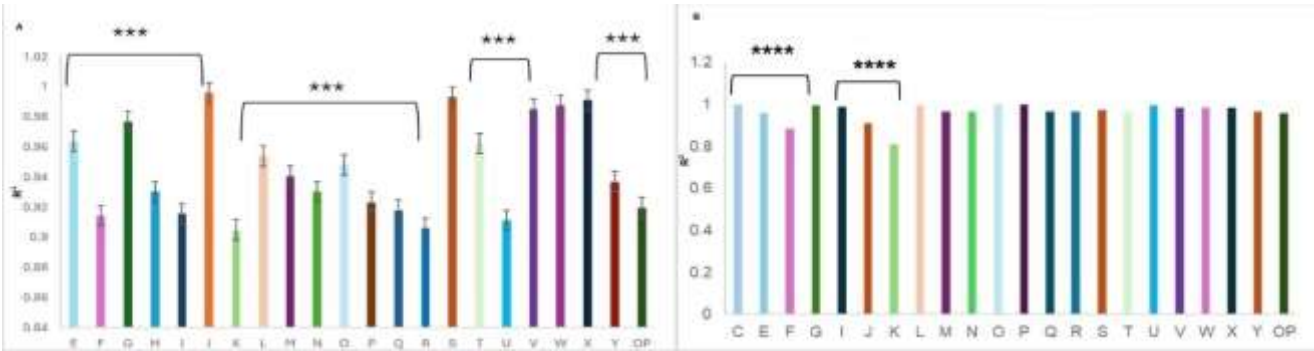


Figure 7: Statistical analysis of R² value of release Korsmeyer Peppas kinetic model of hydrogels(A) and Herchel Bulkley rheological model of hydrogel formulations (B)

Table 6: Results of model fitting of release kinetics of CV-N from CV-N/TFV hydrogel formulation in simulated vaginal fluid pH 4.2.

Kinetic model	Parameter	OPTIMIZED HYDROGEL
Zero order	R ²	0.9355
	K ₀	101.91
First order	R ²	0.7774
	K	0.0033
Korsmeyer-Peppas	R ²	0.9289
	N	1.3461
Higuchi	R ²	0.9822
	K _H	4.6341

Where K₀ is the release constant, R² is the coefficient of determination, K_H is the Higuchi release constant, N is the Higuchi dissolution constant.

Conclusion

The Tenofovir/Cyanovirin-N hydrogel formulation shows strong potential as an on-demand multipurpose preventive technology (MPT) due to its favorable physicochemical properties. Its shear-thinning behavior enhances ease of application and user comfort, promoting acceptance and adherence across varied social and cultural settings. The formulation's smooth, adaptable texture reduces discomfort during use, encouraging consistent application, particularly in communities where cultural sensitivity or stigma may affect the acceptance of vaginal products. High mucoadhesion (≥85%, with optimized formulation at 96.4%) ensures effective retention in the vaginal mucosa, preventing wash-off and supporting prolonged drug contact. The rapid, complete burst release of tenofovir and Cyanovirin-N delivers immediate therapeutic concentrations, offering prompt protection against HIV, HPV, and HSV infections—ideal for on-demand use before or shortly after exposure. While individual agents have shown efficacy in previous studies, further research on the combined TFV/CV-N hydrogel in animal models is crucial for clinical translation.

Conflict of Interest

The author`s declare no conflict of interest.

Authors’ Declaration

The authors hereby declare that the work presented in this article is original and that any liability for claims relating to the content of this article will be borne by them.

Acknowledgments

The authors would like to thank BARC, India for donating the Cyanovirin-N used for this study, MEDAFRICA GMP Laboratory, University of Lagos as well as the entire staff of Pharmaceuticals and Pharmaceutical Technology Department, Faculty of Pharmacy, University of Lagos.

Funding

Cyanovirin-N was supplied by the BARC group, Mumbai, India. Some materials were funded by MEDAFRICA Foundation Inc. Scotch Plains, NJ, USA award number 01/2021/22.

References

1. Thang, N. H., Chien, T. B.,Cuong, D. X. Polymer-Based Hydrogels Applied in Drug Delivery: An Overview. Gels, 2023; 9(7): 523. <https://doi.org/10.3390/gels9070523>
2. Vigata, M., Meinert, C., Hutmacher, D. W., Bock, N. Hydrogels as Drug Delivery Systems: A Review of Current Characterization and Evaluation Techniques. Pharmaceutics, 2020; 12(12): 1188. <https://doi.org/10.3390/pharmaceutics12121188>
3. Mehta, P., Sharma, M., Devi, M. Hydrogels: An overview of its classifications, properties, and applications. J. Mech. Behav. Biomed. Mater., 2023; 147: 106145. <https://doi.org/10.1016/j.jmbbm.2023.106145>
4. Trujillo, S., Gonzalez-Garcia, C., Rico, P., Reid, A., Windmill, J., Dalby, M. J., Salmeron-Sanchez, M. Engineered 3D hydrogels with full-length fibronectin that sequester and present growth factors. Biomaterials, 2020;

- 252: 120104.
<https://doi.org/10.1016/j.biomaterials.2020.120104>
5. Zhu, S., Li, Y., He, Z., Ji, L., Zhang, W., Tong, Y., Luo, J., Yu, D., Zhang, Q., Bi, Q. Advanced injectable hydrogels for cartilage tissue engineering. *Front. biotechnol.*, 2022; 10: 954501.
<https://doi.org/10.3389/fbioe.2022.954501>
 6. Ho, T.-C., Chang, C.-C., Chan, H.-P., Chung, T.-W., Shu, C.-W., Chuang, K.-P., Duh, T.-H., Yang, M.-H., Tyan, Y.-C. Hydrogels: Properties and Applications in Biomedicine. *Molecules*, 2022; 27(9): 2902.
<https://doi.org/10.3390/molecules27092902>
 7. Gosecka, M., & Gosecki. Antimicrobial Polymer-Based Hydrogels for the Intravaginal Therapies-Engineering Considerations. *Pharmaceutics*, 2021; 13(9): 1393.
<https://doi.org/10.3390/pharmaceutics13091393>
 8. Chaitanya M., Dhairya J., Siddhesh S., Pramila M., Upendra K., Subrata BG., Sanchita BG. Effect of salt addition towards enhancement of water retention capacity of hydrogel. *Mater. Today: Proc.*, 2024; 2214-7853.
<https://doi.org/10.1016/j.matpr.2024.05.072>
 9. Osmalek, T., Froelich, A., Jadach, B., Tatarek, A., Gadziński, P., Falana, A., Gralińska, K., Ekert, M., Puri, V., Wrotyńska-Barczyńska, J., Michniak-Kohn, B. Recent Advances in Polymer-Based Vaginal Drug Delivery Systems. *Pharmaceutics*, 2021; 13(6): 884.
<https://doi.org/10.3390/pharmaceutics13060884>
 10. Antimisariis, S. G., Mourtas, S. Recent advances on anti-HIV vaginal delivery systems development. *Adv. Drug Deliv. Rev.*, 2015; 92: 123–145.
<https://doi.org/10.1016/j.addr.2015.03.015>
 11. Cook, M. T., Brown, M. B. Polymeric gels for intravaginal drug delivery. *JCR.*, 2018; 270: 145–157.
<https://doi.org/10.1016/j.jconrel.2017.12.004>
 12. Chang, LC, Bewley, C. Potent Inhibition of HIV-1 Fusion by Cyanovirin-N Requires Only a Single High Affinity Carbohydrate Binding Site: Characterization of Low Affinity Carbohydrate Binding Site Knockout Mutants. *J Mol Biol.*, 2002; 318: 1–8. [https://doi.org/10.1016/S0022-2836\(02\)00045-1](https://doi.org/10.1016/S0022-2836(02)00045-1)
 13. Tsai CC, Emau P, Jiang Y, Agy MB, Shattock RJ, Schmidt A, Morton WR, Gustafson KR, Boyd MR. Cyanovirin-N inhibits AIDS virus infections in vaginal transmission models. *AIDS Res. Hum. Retrovir.*, 2004; 20(1):11–8. DOI: [10.1089/088922204322749459](https://doi.org/10.1089/088922204322749459)
 14. Yu, H., Liu, Z., Lv, R., Zhang, W. Antiviral activity of recombinant cyanovirin-N against HSV-1. *Viro. Sin.*, 2010; 25(6), 432–439. <https://doi.org/10.1007/s12250-010-3131-3>
 15. Mazalovska M, Kouokam JC. Lectins as Promising Therapeutics for the Prevention and Treatment of HIV and Other Potential Coinfections. *Biomed Res Int.*, 2018; 8: 3750646. Available from: <https://www.ncbi.nlm.nih.gov/pmc/articles/PMC5964492/>
 16. Dey B, Lerner DL, Lusso P, Boyd MR, Elder JH, Berger EA. Multiple Antiviral Activities of Cyanovirin-N: Blocking of Human Immunodeficiency Virus Type 1 gp120 Interaction with CD4 and Coreceptor and Inhibition of Diverse Enveloped Viruses. *J Virol.* 2000; 74(10): 4562–4569. <https://journals.asm.org/doi/pdf/10.1128/jvi.74.10.4562-4569.2000>
 17. Wassner C, Bradley N, Lee Y. A Review and Clinical Understanding of Tenofovir: Tenofovir Disoproxil Fumarate versus Tenofovir Alafenamide. *J Int Assoc Provid AIDS Care.* 2020; 19: 2325958220919231.
 18. Abdool Karim SS, Abdool Karim Q, Kharsany ABM, Baxter C, Grobler AC, Werner L, Kashuba A, Mansoor LE, Samsunder N, Mindel A, Gengiah TN, CAPRISA 004 Trial Group. Tenofovir Gel for the Prevention of Herpes Simplex Virus Type 2 Infection. *N Engl J Med.*, 2015. <https://doi.org/10.1056/NEJMoa1410649>.
 19. Marrazzo, JM., Rabe, L., Kelly, C., Richardson, B., Deal, C., Schwartz, JL., Chirenje, ZM., Piper, J., Morrow, RA., Hendrix, CW., Marzinke, MA., Hillier, SL. Tenofovir Gel for Prevention of Herpes Simplex Virus Type 2 Acquisition: Findings from the VOICE Trial. *J Infect Dis.*, 2019; 219(12): 1940–1947. <https://doi.org/10.1093/infdis/jiz045>
 20. Inada, K., Kaneko, S., Kurosaki, M., Yamashita, K., Kirino, S., Osawa, L., Hayakawa, Y., Sekiguchi, S., Higuchi, M., Takaura, K., Maeyashiki, C., Tamaki, N., Yasui, Y., Itakura, J., Takahashi, Y., Tsuchiya, K., Nakanishi, H., Okamoto, R., Izumi, N. Tenofovir alafenamide for prevention and treatment of hepatitis B virus reactivation and de novo hepatitis. *JGH Open.*, 2021; 5(9): 1085–1091.
<https://doi.org/10.1002/jgh3.12636>
 21. Patel, SK., Agashe, H., Patton, DL., Sweeney, Y., Beamer, MA., Hendrix, CW., Hillier, SL., Rohan, LC. Tenofovir vaginal film as a potential MPT product against HIV-1 and HSV-2 acquisition: Formulation development and preclinical assessment in non-human primates. *Front. Reprod. Health.*, 2023; 5. <https://doi.org/10.3389/frph.2023.1217835>
 22. Holt BY, Turpin JA, Romano J. Multipurpose Prevention Technologies: Opportunities and Challenges to Ensure Advancement of the Most Promising MPTs. *Front Reprod Health.*, 2021; 3: 704841.
<https://pmc.ncbi.nlm.nih.gov/articles/PMC9580637/>
 23. Gupta SK, Deshpande AP, Kumar R. Rheological and dielectric behavior of sodium carboxymethyl cellulose (NaCMC)/Ca²⁺ and esterified NaCMC/Ca²⁺ hydrogels: Correlating microstructure and dynamics with properties. *Carbohydr Polym.*, 2024; 335: 122049. <https://doi.org/10.1016/j.carbpol.2024.122049>
 24. Akil A, Agashe H, Dezzutti CS, Moncla BJ, Hillier SL, Devlin B, Shi Y, Uranker K, Rohan LC. Formulation and characterization of polymeric films containing combinations of antiretrovirals (ARVs) for HIV prevention. *Pharm Res.* 2015 ;32(2):458-468. doi: [10.1007/s11095-014-1474-4](https://doi.org/10.1007/s11095-014-1474-4)
 25. Parhi R. Cross-Linked Hydrogel for Pharmaceutical Applications: A Review. *Adv Pharm Bull.*, 2017; 7(4): 515–530. DOI: [10.15171/apb.2017.064](https://doi.org/10.15171/apb.2017.064)
 26. Agarwal R, Trivedi J, Mitra D. High yield production of recombinant Cyanovirin-N (antiviral lectin) exhibiting significant anti-HIV activity, from a rationally selected *Escherichia coli* strain. *Process Biochem* 2020; 93:1–11. <https://www.sciencedirect.com/science/article/pii/S1359511320300775>
 27. Cao H, Duan L, Zhang Y, Cao J, Zhang K. Current hydrogel advances in physicochemical and biological response-driven biomedical application diversity. *Signal Transduct Target Ther.* 2021;6(1):426. DOI: [10.1038/s41392-021-00830-x](https://doi.org/10.1038/s41392-021-00830-x)
 28. Oyediran KO, Cardoso-Daodu IM, Bassey PO, Ogundemuren DA, Muhammed R, Ojo EO, Amenaghawon AN, Azubuike CP, Agarwal R, Haritha K, Ilomunaya MO. Artificial Neural Network guided optimization of Tenofovir and Cyanovirin-N multipurpose preventive hydrogel formulation developed using the Box Behnken design model. *PHSA*, 2025; 100079; 2773-2169. <https://doi.org/10.1016/j.pscia.2025.100079>
 29. The European Agency for the Evaluation of Medicinal Products, Human Medicines Evaluation Unit (International conference of Harmonization (ICH). Stability Testing of New Drug Substances and Products, ICH Harmonised Tripartite Guideline. ICH- Technical Coordination- R. Bass 1993. <http://www.pharma.gally.ch/ich/q1a038095en.pdf>
 30. Bhattad, A. Review on viscosity measurement: devices, methods and models. *J Therm Anal Calorim.* 2023; 148, 6527–65432023; 148
 31. May, CJ., Henderson, KO. Rheological Measurement Methods and Equipment. In: Wang, Q.J., Chung, YW. (eds) *Encyclopedia of Tribology*. Springer. 2013. https://doi.org/10.1007/978-0-387-92897-5_969

32. Ilomuanya, MO., Elesho, RF., Amenaghawon, AN., Adetuyi, AO., Velusamy, V., Akanmu, AS. Development of trigger sensitive hyaluronic acid/palm oil-based organogel for in vitro release of HIV/AIDS microbicides using artificial neural networks. *FJPS.*, 2020; 6(1): 1. <https://doi.org/10.1186/s43094-019-0015-8>
33. Hamed, R., AbuRezeq, A., Tarawneh, O. Development of hydrogels, oleogels, and bigels as local drug delivery systems for periodontitis. *Drug Dev Ind Pharm.*, 2018; 44(9): 1488–1497. <https://doi.org/10.1080/03639045.2018.1464021>
34. Owen, DH., Katz, DF. A vaginal fluid simulant. *Contraception* 1999; 59(2), 91–95. [https://doi.org/10.1016/s0010-7824\(99\)00010-4](https://doi.org/10.1016/s0010-7824(99)00010-4)
35. Chimpiri, S., Sowmya, D., Murthy, V., Rani, A. Development and validation of stability indicating UV-spectrophotometric method for the estimation of tenofovir in its bulk and pharmaceutical dosage form. 2015; 7, 177–185.
36. Lowry, OH., Rosebrough, NJ., Farr, AL., Randall, RJ. Protein measurement with the Folin phenol reagent. *J Biol Chem.*, 1951; 193(1): 265–275.
37. Bashir S, Hina M, Iqbal J, Rajpar AH, Mujtaba MA, Alghamdi NA, Wageh S, Ramesh K, Ramesh S. Fundamental Concepts of Hydrogels: Synthesis, Properties, and Their Applications. *Polymers (Basel)*. 2020; 12(11): 2702. Doi: [10.3390/polym12112702](https://doi.org/10.3390/polym12112702)
38. Stojkov, G., Niyazov, Z., Picchioni, F., Bose, R. K. Relationship between Structure and Rheology of Hydrogels for Various Applications. *Gels* 2021; 7(4): 255. <https://doi.org/10.3390/gels7040255>
39. Robinson KA, Meuse CW. Deep hydration: Poly(ethylene glycol) Mw 2000–8000 Da probed by vibrational spectrometry and small-angle neutron scattering and assignment of ΔG° to individual water layers. *Polymer* 2013; 54: 2: 709–723. Doi: <https://doi.org/10.1016/j.polymer.2012.11.016>
40. Mohammed, MI., El-Sayed, F. PEG's impact as a plasticizer on the PVA polymer's structural, thermal, mechanical, optical, and dielectric characteristics. *Opt Quant Electron.*, 2023; 55: 1141. Doi: <https://doi.org/10.1007/s11082-023-05420-5>
41. Li, X., Gong, J. P. Design principles for strong and tough hydrogels. *Nat. Rev. Mater.*, 2024; 9(6): 380–398. <https://doi.org/10.1038/s41578-024-00672-3>
42. Kopač, T., Ručigaj, A., Krajnc, M. The mutual effect of the crosslinker and biopolymer concentration on the desired hydrogel properties. *Int. J. Biol. Macromol* 2020; 159: 557–569. <https://doi.org/10.1016/j.ijbiomac.2020.05.088>
43. Real, L. E. P. Degradation and Stabilization of Polymers. In L. E. P. Real (Ed.). *Weathering of Polymers and Plastic Materials* (pp. 1–33). *Springer Nature Switzerland* 2023. https://doi.org/10.1007/978-3-031-33285-2_1
44. Nair, R., Roy Choudhury, A. Synthesis and rheological characterization of a novel shear thinning levan gellan hydrogel. *Int. J. Biol. Macromol.*, 2020; 159: 922–930. <https://doi.org/10.1016/j.ijbiomac.2020.05.119>
45. Fan Z, Cheng P, Zhang P, Zhang G, Han J. Rheological insight of polysaccharide/protein-based hydrogels in recent food and biomedical fields: A review. *Int. J. Biol. Macromol.*, 2022; 222: B: 1642–1664. <https://doi.org/10.1016/j.ijbiomac.2022.10.082>
46. Aposporidis A, Haber E, Olshanskii MA, Veneziani A. A mixed formulation of the Bingham fluid flow problem: Analysis and numerical solution. *Comput. Methods Appl. Mech. Eng.*, 2011; 200: 2434–2446. Doi: <https://doi.org/10.1016/j.cma.2011.04.004>
47. Mullineux G. Non-linear least squares fitting of coefficients in the Herschel–Bulkley model. *Appl. Math. Model.*, 2008; 32(12): 2538–2551. <https://doi.org/10.1016/j.apm.2007.09.010>
48. Shaikh, R., Raj Singh, TR., Garland, MJ., Woolfson, AD., Donnelly, RF. Mucoadhesive drug delivery systems. *J Pharm Bioallied Sci.*, 2011; 3(1): 89–100. <https://doi.org/10.4103/0975-7406.76478>
49. Lacroix, G., Gouyer V, Gottrand, F, Desseyn, JL. The Cervicovaginal Mucus Barrier. *Int. J. Mol. Sci.*, 2020; 21(21): 8266. <https://doi.org/10.3390/ijms21218266>
50. Peppas, NA., Huang, Y. Nanoscale technology of mucoadhesive interactions. *Adv. Drug Deliv. Rev.*, 2004; 56(11): 1675–1687. <https://doi.org/10.1016/j.addr.2004.03.001>
51. Hezaveh, H, Muhamad, I, Noshadi, I, Fen, L, Ngadi, N. Swelling behavior and controlled drug release from cross-linked carrageenan/NaCMC hydrogel by diffusion mechanism. *J. Microencapsul.*, 2012; 29: 368–379. Doi: [10.3109/02652048.2011.651501](https://doi.org/10.3109/02652048.2011.651501)
52. Talevi, A., Ruiz, M.E. Korsmeyer-Peppas, Peppas-Sahlin, and Brazel-Peppas: Models of Drug Release. In: *The ADME Encyclopedia*. Springer, Cham., 2021. https://doi.org/10.1007/978-3-030-51519-5_35-1
53. Roy, S., Pal, K., Anis, A., Pramanik, K., Prabhakar, B. Polymers in Mucoadhesive Drug-Delivery Systems: A Brief Note. *Des. Monomers Polym.*, 2009; 12(6): 483–495. <https://doi.org/10.1163/138577209X12478283327236>